Differential-Transfer-Matrix Based on Airy's Functions in Analysis of Planar Optical Structures With Arbitrary Index Profiles

Nima Zariean, Peyman Sarrafi, Khashayar Mehrany, and Bizhan Rashidian

***Abstract*—A novel analytical method for solution of planar optical structure with arbitrary refractive index profile is proposed. This new method is founded on differential-transfer-matrices, whose field solutions are based on Airy's trial functions. In contrast to conventional Wentzel, Kramers, and Brillouin (WKB) solutions, which diverge around the turning points, this approach can be successfully used for exact calculation of various functions, including eigenvalues of optical waveguides with arbitrary index profiles, and complex reflection and transmission coefficients, even at the presence of turning points. The method is rigorous and can be applied for both major polarizations.**

***Index Terms*—Airy functions, differential-transfer-matrix, graded-index profiles, planar waveguide, Wentzel, Kramers, and Brillouin (WKB) method.**

I. Introduction

THANKS to the exponential growth of the fast computers and large memories, numerical methods are undoubtedly today's most convenient techniques to analyze different photonic devices and components. These methods cannot, however, impart as much physical insight as closed form expressions and semi-analytical methods usually do. In this respect, different mathematical treatments of optical structures together with their corresponding physical interpretations are still popular with many scientists. Furthermore, measured with the available numerical methods such as the finite element method (FEM), the finite difference time domain method (FDTD), etc., the aforementioned semi-analytical solutions and approximations are much easier to be implemented. Therefore, even though finding an exact solution to either the general form of Schrödinger equation or the Helmholtz wave equation is almost impossible, various closed form approximate solutions attempting to give reasonably accurate results have been so far reported.

Among others, WKB approximation [1]- initially introduced by Wentzel, Kramers, and Brillouin, is one of the most famous approaches of treating Schrödinger–Helmholtz equation. Despite its being widely used, the solution obtained by this method diverges around the turning points and is applicable only to the slowly varying and continuous forms of the potential energy or electric permittivity- depending on the type of the problem at hand. However, its accuracy can be further improved by employing a variational method using WKB expansions as trial functions [2]. This modified approach yields very accurate eigenvalues whenever the turning points are not too close to the region of interest. Furthermore, similar higher order variational method has been adapted for improving the overall accuracy [3].

As for none of the WKB-based methods can properly handle the problem caused by the turning points, a more rigorous approach based on the modified airy functions (MAF) was also introduced. This approach, originally proposed by Langer [4], was later successfully applied to planar optical waveguides and quantum-well structures [5]–[8]. For most of the profiles, the MAF method leads to more accurate results than the WKB. Additionally, it does not suffer from the unwanted divergence around the turning points. However, the latter (MAF) appropriately combined with the former (WKB) is also capable of giving convergent and accurate solutions to miscellaneous cases such as planar optical waveguides, graded index fibers, and the circular slab waveguides [9]–[11].

Differential transfer matrix method (DTMM), being based on WKB-like basis functions, has also been reported to analyze inhomogeneous yet arbitrary optical structures [12], [13]. Much like the original WKB method, DTMM diverges around the turning points and cannot successfully yield accurate eigenvalues. In this manuscript, however, electromagnetic fields are expanded in terms of Airy's functions and a novel type of differential-transfer-matrix is given. This newly differential-transfer-matrix faces no numerical difficulty around the turning points and consequently yields accurate numerical results. In contrast to most of the conventional approximate solutions, the proposed method separately treats the TM as well as the TE polarized waves.

The structure of this manuscript is as follows: the formulation of the proposed method for both major polarizations, TE and TM, is presented in Section II. In Section III, the affinity of the proposed method with differential averaging in piecewise linear media is discussed to provide some further insight about the nature of the proposed formulation. Various numerical examples are presented in Section IV. Finally, conclusions are made in Section V.

Manuscript received May 21, 2007; revised August 28, 2007. This work was supported in part by ITRC.

The authors are with the School of Electrical Engineering, Sharif University of Technology, Tehran 11365-8639, Iran (e-mail: nima_z@ee.sharif.edu; sarrafi@ee.sharif.edu; mehrany@sharif.edu; rashidia@sharif.edu).

Digital Object Identifier 10.1109/JQE.2007.912469

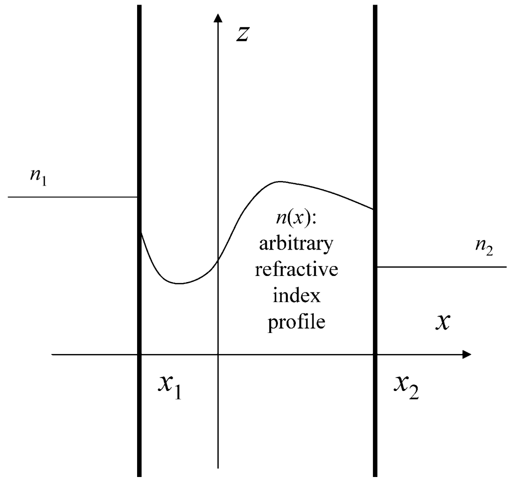

Fig. 1. Illustration of the inhomogeneous optical structure used in examples.

II. Formulation

A. TE Polarization

Consider a one-dimensional isotropic, lossless, and non-magnetic inhomogeneous structure, shown in Fig. 1. For such a structure, the tangential electric (y -component) and magnetic (z -component) fields may be expressed as

$$E_y = S_{\mathrm{TE}}(x)\exp(-jk_z z) \quad (1a)$$

$$-j\left(\frac{\mu_0}{\varepsilon_0}\right)^{\frac{1}{2}} H_z = U_{\mathrm{TE}}(x)\exp(-jk_z z) \quad (1b)$$

where $S_{\mathrm{TE}}(x), U_{\mathrm{TE}}(x)$, and k_z represent the tangential electric field amplitude, normalized tangential magnetic field amplitude, and wavenumber in the z direction, respectively.

Substituting (1) into Maxwell's equations and eliminating the normal (x) component of the magnetic field, a set of coupled-wave equations is found and can be written in a matrix form

$$M_{\mathrm{TE}}(x) = k_0 \begin{bmatrix} 0 & 1 \\ -n^2(x) + \left(\frac{k_z}{k_0}\right)^2 & 0 \end{bmatrix} \quad (2a)$$

$$\frac{d}{dx}\begin{bmatrix} S_{\mathrm{TE}} \\ U_{\mathrm{TE}} \end{bmatrix} = M_{\mathrm{TE}}(x)\begin{bmatrix} S_{\mathrm{TE}} \\ U_{\mathrm{TE}} \end{bmatrix}. \quad (2b)$$

Now, the normalized tangential electromagnetic fields, i.e., $S_{\mathrm{TE}}(x)$ and $U_{\mathrm{TE}}(x)$ can be rewritten in terms of two new parameters $A(x)$ and $B(x)$

$$\begin{bmatrix} S_{\mathrm{TE}}(x) \\ U_{\mathrm{TE}}(x) \end{bmatrix} = Q_{\mathrm{TE}}(x)\begin{bmatrix} A(x) \\ B(x) \end{bmatrix} \quad (3)$$

where $Q_{\mathrm{TE}}(x)$ is defined as

$$Q_{\mathrm{TE}}(x) = \begin{bmatrix} Ai(\xi) & Bi(\xi) \\ \frac{\left(-\frac{d}{dx}k^2\right)^{1/3} Ai'(\xi)}{k_0} & \frac{\left(-\frac{d}{dx}k^2\right)^{1/3} Bi'(\xi)}{k_0} \end{bmatrix} \quad (4a)$$

$$\xi(x) = \frac{-k^2(x)}{\left(-\frac{d}{dx}k^2(x)\right)^{2/3}}. \quad (4b)$$

Prime denotes the differentiation with respect to ξ and $k(x)$ represents the wevenumber in the x direction and is defined as $k(x) = k_0\sqrt{n^2(x) - N^2}$ with $N = k_z/k_0$.

Here, the basis functions $Ai(x)$ and $Bi(x)$ represent the Airy's functions of the first and second kind respectively, and are the solutions of the following equation:

$$\frac{d^2\psi}{dx^2} - x\,\psi = 0. \quad (5)$$

It should be noticed that these basis functions satisfy the second order Helmholtz equation of a medium in which the wevenumber in the x direction, i.e., $k(x)$ varies linearly. This is in contrast to the WKB-like basis functions, i.e., forward and backward plane waves, which satisfy the second order wave equation of a medium in which $k(x)$ is almost constant. Therefore, these basis functions allow us to reasonably approximate harsher variations of $k(x)$ within the medium.

Now by using (3) one can write down

$$\frac{d}{dx}\begin{bmatrix} S_{\mathrm{TE}} \\ U_{\mathrm{TE}} \end{bmatrix} = \frac{dQ_{\mathrm{TE}}}{dx}\begin{bmatrix} A \\ B \end{bmatrix} + Q_{\mathrm{TE}}\frac{d}{dx}\begin{bmatrix} A \\ B \end{bmatrix} \quad (6)$$

where combining (2) and (6) together with some algebraic manipulation leads to

$$\frac{d}{dx}\begin{bmatrix} A \\ B \end{bmatrix} = W_{\mathrm{TE}}(x)\begin{bmatrix} A \\ B \end{bmatrix} \quad (7)$$

in which

$$W_{\mathrm{TE}}(x) = Q_{\mathrm{TE}}^{-1} M_{\mathrm{TE}} Q_{\mathrm{TE}} - Q_{\mathrm{TE}}^{-1}\frac{d}{dx}Q_{\mathrm{TE}}. \quad (8)$$

The state matrix W_{TE} serves as a novel differential-transfer matrix to obtain the overall transfer matrix

$$\begin{bmatrix} A(x_2) \\ B(x_2) \end{bmatrix} = \exp\left(\int_{x_1}^{x_2} W_{\mathrm{TE}} dx\right)\begin{bmatrix} A(x_1) \\ B(x_1) \end{bmatrix}. \quad (9)$$

This combined with (3) now links the tangential electromagnetic fields at x_2, i.e., $S_{\mathrm{TE}}(x_2)$ and $U_{\mathrm{TE}}(x_2)$, and at x_1, i.e., $S_{\mathrm{TE}}(x_1)$ and $U_{\mathrm{TE}}(x_1)$, together

$$\begin{bmatrix} S_{\mathrm{TE}}(x_2) \\ U_{\mathrm{TE}}(x_2) \end{bmatrix} = Q_{\mathrm{TE}}(x_2)\exp\left(\int_{x_1}^{x_2} W_{\mathrm{TE}} dx\right) Q_{\mathrm{TE}}(x_1)^{-1} \times \begin{bmatrix} S_{\mathrm{TE}}(x_1) \\ U_{\mathrm{TE}}(x_1) \end{bmatrix}. \quad (10)$$

B. TM Polarization

Once again, in the aforementioned inhomogeneous layer, normalized tangential electromagnetic field amplitudes, i.e., $U_{\mathrm{TM}}(x)$ and $S_{\mathrm{TM}}(x)$, can be formulated as

$$H_y = S_{\mathrm{TM}}(x)\exp(-jk_z z) \quad (11a)$$

$$j\left(\frac{\varepsilon_0}{\mu_0}\right)^{\frac{1}{2}} E_z = U_{\mathrm{TM}}(x)\exp(-jk_z z). \quad (11b)$$

Similarly, substitution of (11) into the Maxwell's equations and elimination of the normal component (x) of the electric field, yields the following set of coupled-wave equations:

$$M_{\rm TM}(x) = k_0 \begin{bmatrix} 0 & n^2(x) \\ -1+\frac{1}{n^2(x)}(\frac{k_z}{k_0})^2 & 0 \end{bmatrix} \tag{12a}$$

$$\frac{d}{dx}\begin{bmatrix} S_{\rm TM} \\ U_{\rm TM} \end{bmatrix} = M_{\rm TM}(x)\begin{bmatrix} S_{\rm TM} \\ U_{\rm TM} \end{bmatrix} \tag{12b}$$

where $Q_{\rm TM}(x)$ reads as (13), shown at the bottom of the page. Here

$$r(x) = k^2(x) - 2\left(\frac{n'}{n}\right)^2 + \frac{n''}{n} \tag{14a}$$

$$\zeta(x) = \frac{-r(x)}{\left(-\frac{d}{dx}r(x)\right)^{2/3}}. \tag{14b}$$

Now, the overall transfer matrix of the medium can be obtained in a similar fashion, where the tangential electromagnetic fields at x_2, i.e., $S_{\rm TM}(x_2)$ and $U_{\rm TM}(x_2)$, and at x_1, i.e., $S_{\rm TM}(x_1)$ and $U_{\rm TM}(x_1)$, are related according to the following equations:

$$\frac{d}{dx}\begin{bmatrix} A \\ B \end{bmatrix} = W_{\rm TM}(x)\begin{bmatrix} A \\ B \end{bmatrix}, \tag{15}$$

in which

$$W_{\rm TM}(x) = Q_{\rm TM}^{-1}M_{\rm TM}Q_{\rm TM} - Q_{\rm TM}^{-1}\frac{d}{dx}Q_{\rm TM} \tag{16}$$

and consequently

$$\begin{bmatrix} S_{\rm TM}(x_2) \\ U_{\rm TM}(x_2) \end{bmatrix} = Q_{\rm TM}(x_2) \times \exp\left(\int_{x_1}^{x_2} W_{\rm TM}dx\right) Q_{\rm TM}(x_1)^{-1}\begin{bmatrix} S_{\rm TM}(x_1) \\ U_{\rm TM}(x_1) \end{bmatrix}. \tag{17}$$

C. Extraction of Eigenmodes

The preceding transfer matrix formulation provides an easy way to extract bounded states and eigenmodes. The fields tangential to the boundaries at $x = x_1$ and $x = x_2$ are related via the following matrix product:

$$\begin{bmatrix} S(x_2) \\ U(x_2) \end{bmatrix} = \mathbf{Y}\begin{bmatrix} S(x_1) \\ U(x_1) \end{bmatrix} \tag{18}$$

where $\mathbf{Y}$ denotes the transfer matrix given in (10) and (17) for the TE polarized and TM polarized waves, respectively. Now, the tangential fields corresponding to bounded modes must be exponentially decaying for $x < x_1$

$$S(x) = A_1\exp(\gamma_1(x-x_1)) \tag{19a}$$

$$U(x) = A_1\frac{\gamma_1}{k_0 n_1^{2f}}\exp(\gamma_1(x-x_1)) \tag{19b}$$

and for $x > x_2$

$$S(x) = A_2\exp(-\gamma_2(x-x_2)) \tag{19c}$$

$$U(x) = -A_2\frac{\gamma_2}{k_0 n_2^{2f}}\exp(-\gamma_2(x-x_2)) \tag{19d}$$

where $\gamma_j = k_0\sqrt{N^2 - n_j^2}$ and f reads as 0 for TE polarized waves and 1 for TM polarized waves.

Therefore, (18) can be rewritten as

$$\begin{bmatrix} A_2 \\ -\frac{\gamma_2}{k_0 n_2^{2f}}A_2 \end{bmatrix} = \mathbf{Y}\begin{bmatrix} A_1 \\ \frac{\gamma_1}{k_0 n_1^{2f}}A_1 \end{bmatrix}. \tag{20}$$

Further simplifications of the preceding equation results in the following matrix product:

$$\begin{bmatrix} y_{11}+y_{12}\frac{\gamma_1}{k_0 n_1^{2f}} & -1 \\ y_{21}+y_{22}\frac{\gamma_1}{k_0 n_1^{2f}} & \frac{\gamma_2}{k_0 n_2^{2f}} \end{bmatrix}\begin{bmatrix} A_1 \\ A_2 \end{bmatrix} = \begin{bmatrix} 0 \\ 0 \end{bmatrix} \tag{21}$$

whose determinant must be zero to support bounded states. Here, y_{ij} stands for the ijth element of the $\mathbf{Y}$ matrix.

D. Calculation of Reflection Coefficient

The same procedure can be followed to obtain the reflection and transmission coefficients of incident electromagnetic fields for both major polarizations.

For a case of a plane wave incident from left, i.e., $x < x_1$, normalized incident, reflected, and transmitted waves- being represented by S_i, S_r, and S_t respectively- are of the following form:

$$S_i = \exp(-jk_{x_1}(x-x_1)) \tag{22a}$$

$$S_r = R\exp(jk_{x_1}(x-x_1)) \tag{22b}$$

$$S_t = T\exp(-jk_{x_1}(x-x_2)) \tag{22c}$$

where $k_{x_i} = n_i\cos(\theta)$ and θ denotes the angle of incidence.

Now, total tangential electromagnetic fields at the boundaries $x = x_1$ and $x = x_2$ can be written as

$$S(0) = 1 + R \tag{23a}$$

$$U(0) = (1-R)\left(-j\frac{k_{x_1}}{k_0 n_1^{2f}}\right) \tag{23b}$$

$$S(d) = T \tag{23c}$$

$$Q_{\rm TM}(x) = \begin{bmatrix} n(x)Ai(\zeta) & n(x)Bi(\zeta) \\ \frac{n(x)\left(-\frac{d}{dx}r\right)^{1/3}Ai'(\zeta)+n'(x)\,Ai(\zeta)}{n^2(x)\,k_0} & \frac{n(x)\left(-\frac{d}{dx}r\right)^{1/3}Bi'(\zeta)+n'(x)Bi(\zeta)}{n^2(x)\,k_0} \end{bmatrix} \tag{13}$$

$$U(d) = T\left(-j\frac{k_{x_3}}{k_0 n_3^{2f}}\right). \tag{23d}$$

Substituting these four quantities in (18) leads to a linear set of algebraic equations, whose solution for R, i.e., the complex reflection coefficient can be expressed as

$$R = \frac{S_r}{S_i} = -\frac{y_{21} + j\frac{k_{x_3}}{k_0 n_3^{2f}} y_{11} - j\frac{k_{x_1}}{k_0 n_1^{2f}} y_{22} + \frac{k_{x_1}k_{x_3}}{k_0^2 (n_1 n_3)^{2f}} y_{12}}{y_{21} + j\frac{k_{x_3}}{k_0 n_3^{2f}} y_{11} + j\frac{k_{x_1}}{k_0 n_1^{2f}} y_{22} - \frac{k_{x_1}k_{x_3}}{k_0^2 (n_1 n_3)^{2f}} y_{12}}. \tag{24}$$

Again, y_{ij} stands for the ijth element of the $\mathbf{Y}$ matrix.

In a similar fashion, the complex transmission coefficient T can be written down

$$T = \frac{S_t}{S_i} = \frac{2j\frac{k_{x_1}}{k_0 n_1^{2f}}(y_{11}y_{22} - y_{12}y_{21})}{y_{21} + j\frac{k_{x_3}}{k_0 n_3^{2f}} y_{11} + j\frac{k_{x_1}}{k_0 n_1^{2f}} y_{22} - \frac{k_{x_1}k_{x_3}}{k_0^2 (n_1 n_3)^{2f}} y_{12}}. \tag{25}$$

III. Differential Averaging Based on Piecewise Linear Approximation

In this section, the affinity of the proposed approach with analysis of wave propagation by using piecewise linear approximation in analysis of inhomogeneous structures is discussed. The refractive index profile is divided into a number of sections, wherein linear interpolation of $k^2(x)$ is employed as an approximate expression. In this fashion, $k^2(x)$ is assumed to be linear within the $[x_0\Delta x, x_0]$ and $[x_0, x_0+\Delta x]$ intervals. Consequently, $A(x)$ and $B(x)$ will be constants equal to $A(x_0)$ and $B(x_0)$ within the $[x_0\Delta x, x_0]$, and $A(x_0+\Delta x)$ and $B(x_0+\Delta x)$ within the $[x_0, x_0+\Delta x]$. Then the appropriate boundary conditions impose (26a)–(26d), shown at the bottom of the page and $Q_{1\to 2}$ is the transfer matrix across the arbitrary interface x_0. Without loss of generality, (26a) can be written down as follows:

$$\begin{bmatrix} A(x+\Delta x) \\ B(x+\Delta x) \end{bmatrix} = Q_{x\to x+\Delta x}\begin{bmatrix} A(x) \\ B(x) \end{bmatrix}. \tag{27}$$

Now, if $k(x)$, $A(x)$, and $B(x)$ are analytic functions of x, the preceding equation would be further simplified by applying the Taylor series expansion

$$\frac{d}{dx}\begin{bmatrix} A(x) \\ B(x) \end{bmatrix} + \begin{bmatrix} A(x) \\ B(x) \end{bmatrix}\Delta x \approx Q_{x\to x+\Delta x}\begin{bmatrix} A(x) \\ B(x) \end{bmatrix}. \tag{28}$$

Further simplification of this latter equation as Δx tends to zero yields

$$\frac{d}{dx}\begin{bmatrix} A(x) \\ B(x) \end{bmatrix} = \lim_{\Delta x\to 0}\frac{Q_{x\to x+\Delta x} - I}{\Delta x}\begin{bmatrix} A(x) \\ B(x) \end{bmatrix} = W(x)\begin{bmatrix} A(x) \\ B(x) \end{bmatrix}. \tag{29}$$

which brings in the same state matrix as the one already introduced in (8). This approach shows that the mathematical formulation as presented in previous section is strongly connected to wave propagation in piecewise linear media.

IV. Numerical Examples

In this section, different examples are presented to justify the validity of the proposed approach. The examples belong to optical structures; however, by change of dimensions and minor redefinitions of parameters, quantum mechanical systems can be analyzed along the same vein. All these examples are based on two different profiles, both widely studied in literature.

A. Truncated Exponential Index Profile

Consider the structure shown in Fig. 2, which depicts an inhomogeneous refractive index profile of the following form:

$$n(x) = \begin{cases} n_0 \exp\left[\frac{x}{d}\ln\left(\frac{n_s}{n_0}\right)\right] & 0 < x < d \\ n_0 & x < 0 \text{ or } x > d. \end{cases} \tag{30}$$

In Fig. 3, the TE polarized reflection coefficient of the structure is plotted versus normalized frequency. In this calculation, where $n_0 = 2.177$, and $n_s = 2.220$ and the angle of incidence

$$\begin{bmatrix} A(x_0+\Delta x) \\ B(x_0+\Delta x) \end{bmatrix} = Q_{1\to 2}\begin{bmatrix} A(x_0) \\ B(x_0) \end{bmatrix} \tag{26a}$$

$$Q_{1\to 2} = \pi\begin{bmatrix} Ai(\xi_1)Bi'(\xi_2) - \left(\frac{\frac{d}{dx}k^2(x_0)}{\frac{d}{dx}k^2(x_0+\Delta x)}\right)^{\frac{1}{3}} Ai'(\xi_1)Bi(\xi_2) & Bi(\xi_1)Bi'(\xi_2) - \left(\frac{\frac{d}{dx}k^2(x_0)}{\frac{d}{dx}k^2(x_0+\Delta x)}\right)^{\frac{1}{3}} Bi'(\xi_1)Bi(\xi_2) \\ -Ai(\xi_1)Ai'(\xi_2) + \left(\frac{\frac{d}{dx}k^2(x_0)}{\frac{d}{dx}k^2(x_0+\Delta x)}\right)^{\frac{1}{3}} Ai'(\xi_1)Ai(\xi_2) & -Bi(\xi_1)Ai'(\xi_2) + \left(\frac{\frac{d}{dx}k^2(x_0)}{\frac{d}{dx}k^2(x_0+\Delta x)}\right)^{\frac{1}{3}} Bi'(\xi_1)Ai(\xi_2) \end{bmatrix} \tag{26b}$$

$$\xi_1 = -\frac{k^2(x_0)}{\left(-\frac{d}{dx}k^2(x_0)\right)^{\frac{2}{3}}} \tag{26c}$$

$$\xi_2 = -\frac{k^2(x_0+\Delta x) - \frac{d}{dx}k^2(x_0+\Delta x)\,\Delta x}{\left(-\frac{d}{dx}k^2(x_0+\Delta x)\right)^{\frac{2}{3}}} \tag{26d}$$

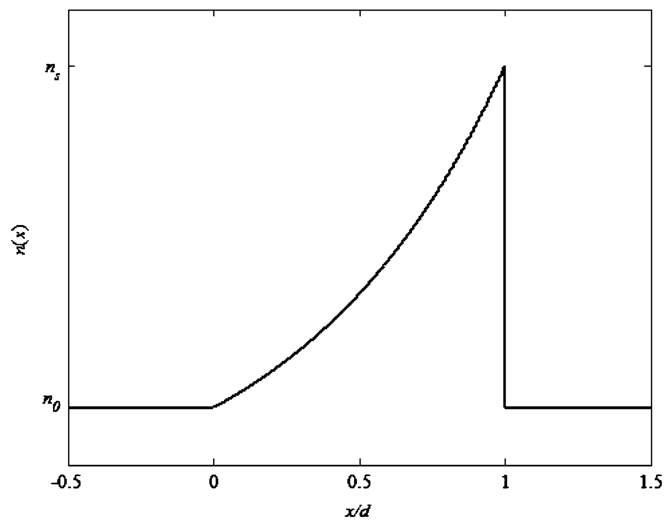

Fig. 2. Exponential index profile plotted versus normalized distance.

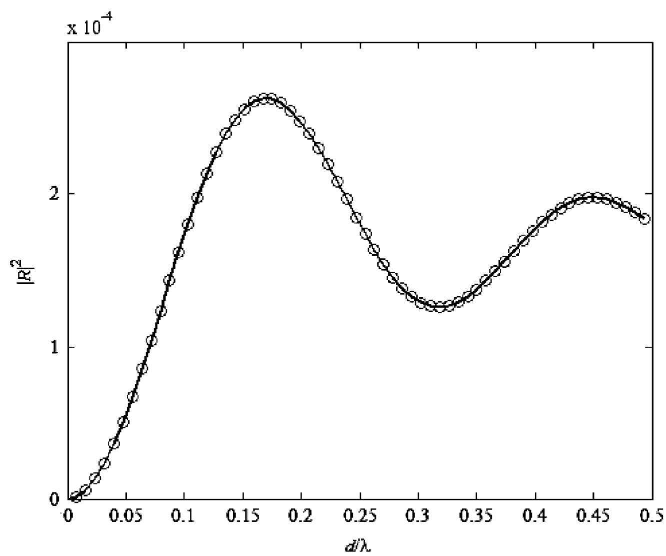

Fig. 3. Reflection coefficient of the structure shown in Fig. 2 with $n_0 = 2.177, n_s = 2.220$, and $\theta = 30°$ for TE polarization. The solid line represents the exact results and the circles stand for the proposed method.

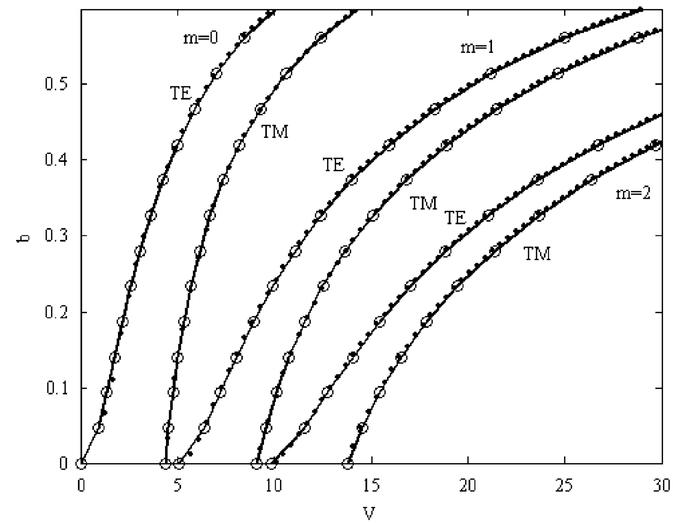

Fig. 4. Dispersion curves of a waveguide with exponential index profile for TE and TM polarizations with $n_0 = 2.177$, and $n_s = 2.220$. Solid line: exact solution; Circles: the proposed method; Dots: polynomial expansion approach.

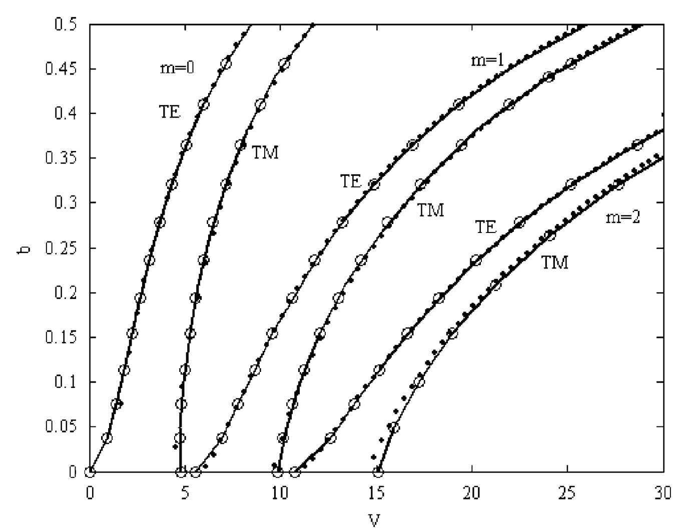

Fig. 5. Dispersion curves of waveguide with exponential index profile for TE and TM polarizations with $n_0 = 2.5$ and $n_s = 3.8$. Solid line: exact solution; circles: the proposed method; dots: polynomial expansion approach.

is 30°, two different approaches are employed. The first, depicted by solid line in the figure, is based on the exact analytical solution, which is available in terms of Bessel functions. The second, plotted via circles, is obtained by following our proposed method and is in good agreement with the exact results.

Furthermore, the bounded eigenmodes supported by this structure are extracted for both major polarizations. This time, the calculations were carried out for two different sets of parameters. First, the values of the parameters are chosen to be $n_0 = 2.177$, and $n_s = 2.220$, where the dispersion diagram of both major polarizations, i.e., normalized propagation constant $\mathrm{b} = (N^2 - n_0^2)/(n_s^2 - n_0^2)$ versus normalized frequency $\mathrm{V} = k_0 d\sqrt{n_s^2 - n_0^2}$, is plotted in Fig. 4. To test the accuracy of the proposed method, two different approaches, i.e., exact analytical solution and polynomial expansion method [14], [15], are employed and an excellent agreement between these different approaches is observed.

Second, the values of the parameters are chosen to be $n_0 = 2.5$, and $n_s = 3.8$. Now as the contrast between n_s and n_0 increases, the accuracy of the presented approach slowly declines. Notwithstanding, such minor errors, which stem from the unrealistically large values of $n_s n_0$, can be easily alleviated by dividing the whole inhomogeneous structure into two cascaded inhomogeneous layers for $0 < x < d/2$ and $d/2 < x < d$. Each one of these inhomogeneous sublayers now enjoys a lower contrast of $n(x)$. By applying this simple technique, the dispersion diagram of both major polarizations for this new case is also plotted in Fig. 5, and once again, the excellent accuracy of the proposed method is demonstrated.

Figs. 3–5 clearly show that the most accurate numerical results as obtained by following the polynomial expansion method and/or finely discretized staircase approximation tally with those calculated by following our proposed method. This

TABLE I
COMPARISON OF RELATIVE ERROR FOR B, NORMALIZED PROPAGATION CONSTANT FOR TRUNCATED EXPONENTIAL PROFILE AT $V = 4.0$ AND (a) $n_0 = 2.177, n_s = 2.220$ AND (b) $n_0 = 2.5, n_s = 3.8$

	Transfer Matrix (50 sublayers)	Airy DTMM (no sublayers)	Airy DTMM (2 sublayers)	Polynomial Expansion
(a)	6.4e-5	2.3e-5	3.5e-6	8.4e-8
(b)	9.1e-5	1.2e-2	1.2e-3	2.4e-8

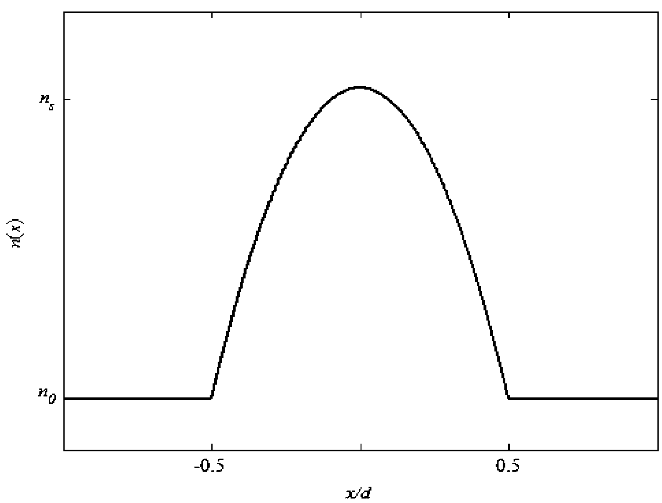

Fig. 6. Parabolic index profile plotted versus normalized distance.

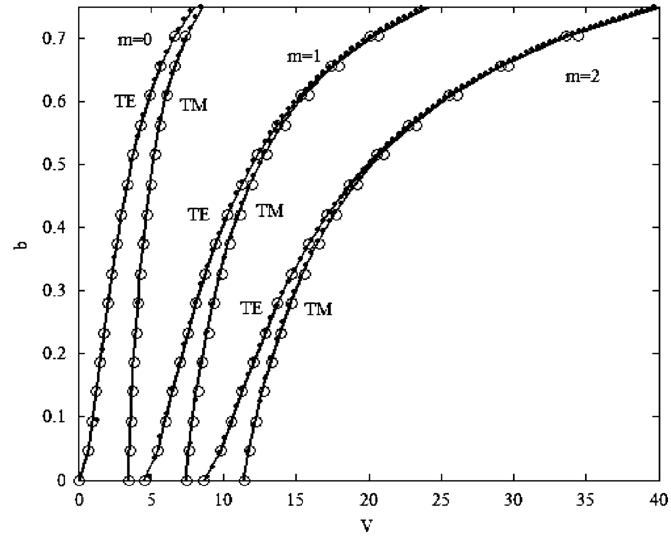

Fig. 7. Dispersion curves of waveguide with exponential index profile for TE and TM polarizations with $n_0 = 2.177$ and $n_s = 2.220$. Solid line: transfer matrix; circles: the proposed method; dots: polynomial expansion approach.

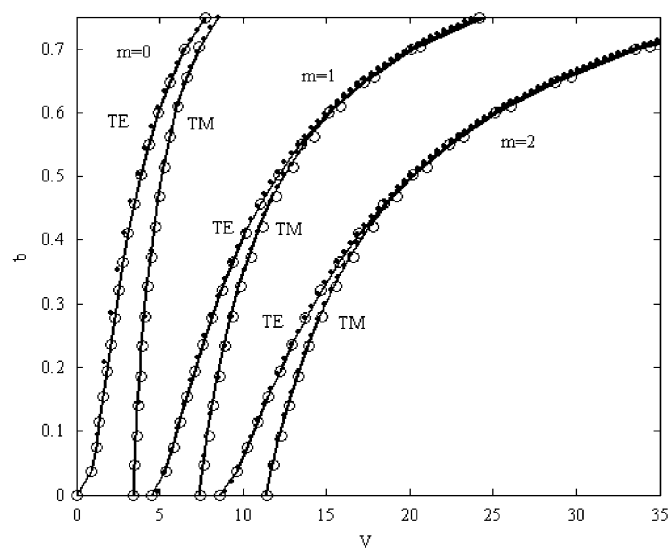

Fig. 8. Dispersion curves of waveguide with exponential index profile for TE and TM polarizations with $n_0 = 2.5$, and $n_s = 3.8$. Solid line: transfer matrix; circles: the proposed method; dots: polynomial expansion approach.

point is further investigated in Table I, where the relative error in calculation of the normalized propagation constants in truncated exponential profiles by using standard transfer matrix method with 50 homogeneous divisions, the polynomial expansion method, and our method without any sublayers and with 2 sublayers are summarized. Transfer matrix method with 4000 subdivisions is employed to calculate the relative error in calculation of normalized propagation constants.

This table clearly demonstrates that the proposed method overpowers the standard transfer matrix method with 50 homogeneous subdivisions in case (a). However, as the contrast between n_s and n_0 is increased in case (b), the accuracy of the presented approach falls off. Yet, this is partially rectified by using two cascaded differential transfer matrices as already proposed. The relative error can be further reduced by using further divisions in cascading Airy-based differential transfer matrices, where 4 sublayers yield the relative error of 3.6e–4 and 8 sublayers yield the relative error of 9.4e–5, comparable to that achieved by transfer matrix method with 50 subdivisions.

B. Symmetric Parabolic Profile

As another example, consider a symmetric parabolic profile, as shown in Fig. 6. index profile for this figure can be given by:

$$n(x) = \begin{cases} \left(n_s^2 - \left(n_s^2 - n_0^2\right)\left(\frac{2x}{d}\right)^2\right)^{1/2}, & -\frac{d}{2} < x < \frac{d}{2} \\ n_0, & x < -\frac{d}{2} \text{ or } x > \frac{d}{2}. \end{cases} \quad (32)$$

As for no analytical closed form expression exists for this index distribution, polynomial expansion method [14], [15], together with the standard transfer matrix method with stair-case approximation of the inhomogeneous refractive index profile [16], are employed to have reference values. Once again, the calculations were carried out for two different sets of parameters: $n_0 = 2.177, n_s = 2.220$, and $n_0 = 2.5, n_s = 3.8$. Dispersion diagrams for these tow different cases are similarly plotted in Figs. 7 and 8, respectively. These figures clearly demonstrate the accuracy of our proposed method.

It should be noticed that the aforementioned technique of cascaded multiple divisions, at virtually no computational cost, is similarly employed to improve the overall accuracy. Here, four subdivisions are employed to calculate the presented results.

V. Conclusion

A mathematically rigorous treatment of inhomogeneous optical structures is presented for both TE and TM polarized waves. In particular, extraction of bounded states and calculation of complex reflection/transmission coefficients are discussed. In contrast to WKB-based solutions, whose accuracy deteriorates for fast refractive index variations or around the turning points, our proposed approach yields very accurate numerical results and encounters no specific numerical difficulty. Although all conducted examples belong to optical structures; by mere change of dimensions and minor redefinitions of parameters, quantum mechanical systems can be similarly analyzed.

References

[1] Merzbacher and Eugen, *Quantum Mechanics*, 3rd ed. New York: Wiley, 1998.

[2] L. Lindbloom and R. T. Robiscoe, “Improving the accuracy of WKB eigenvalues,” *J. Math. Phys.*, vol. 32, no. 5, pp. 1254–1258, May 1991.

[3] V. A. Popescu, “Improving the accuracy of WKB and Langer eigenvalues by higher order variational method,” *Phys. Lett. A*, vol. 349, pp. 220–223, Jan. 2006.

[4] R. E. Langer, “On the asymptotic solutions of ordinary differential equations, with an application to the bessel functions of large order,” *Trans. Amer. Math. Soc.*, vol. 33, pp. 23–64, Jan. 1931.

[5] I. C. Goyal, A. K. Ghatak, and R. L. Gallawa, “An approximate solution to the wave equation-revisited,” *J. Electromagn. Waves Appl.*, vol. 5, pp. 623–636, 1991.

[6] I. C. Goyal, R. L. Gallawa, and A. K. Ghatak, “Methods of analyzing planar optical waveguides,” *Opt. Lett.*, vol. 16, no. 1, pp. 30–32, 1991.

[7] A. K. Ghatak, R. L. Gallawa, and I. C. Goyal, “Accurate solutions to Schrodinger’s equation using modified airy functions,” *IEEE J. Quantum Electron.*, vol. 28, no. 2, pp. 400–403, Feb. 1992.

[8] I. C. Goyal, R. Jindal, and A. K. Ghatak, “Planar optical waveguides with arbitrary index profile: An accurate method of analysis,” *J. Lightw. Technol.*, vol. 15, no. 11, pp. 2179–2182, Nov. 1997.

[9] C.-M. Kim and M.-S. Chung, “Eigenvalue equations of n-parallel graded-index waveguides: WKB analysis,” *IEEE J. Quantum Electron.*, vol. 33, no. 9, pp. 1608–1613, Sep. 1997.

[10] M.-S. Chung and C.-M. Kim, “General eigenvalue equations for optical planar waveguides with arbitrarily graded-index profiles,” *J. Lightw. Technol.*, vol. 18, no. 6, pp. 878–885, Jun. 2000.

[11] C.-M. Kim, Y.-M. Kim, and W.-K. Kim, “Leaky modes of circular slab waveguides: Modified airy functions,” *IEEE J. Sel. Topics Quantum Electron.*, vol. 8, no. 6, pp. 1239–1245, Nov./Dec. 2002.

[12] M. H. Eghlidi, K. Mehrany, and B. Rashidian, “Improved differential-transfer-matrix method for inhomogeneous one-dimensional photonic crystals,” *J. Opt. Soc. Amer. B*, vol. 23, no. 7, Jan. 2006.

[13] M. H. Eghlidi, K. Mehrany, and B. Rashidian, “Modified differential-transfer-matrix method for solution of one-dimensional linear inhomogeneous optical structures,” *J. Opt. Soc. Amer. B*, vol. 22, no. 7, Jul. 2005.

[14] M. Chamanzar, K. Mehrany, and B. Rashidian, “Legendre polynomial expansion for analysis of linear one-dimensional inhomogeneous optical structures and photonic crystals,” *J. Opt. Soc. Amer. B.*, vol. 23, pp. 969–976, 2006.

[15] K. Mehrany and B. Rashidian, “Polynomial expansion of electromagnetic eigenmodes in layered structures,” *J. Opt. Soc. Amer. B.*, vol. 20, pp. 2434–2441, 2003.

[16] A. K. Ghatak, K. Thyagarajan, and M. R. Shenoy, “Numerical analysis of planar optical waveguides using matrix approach,” *J. Lightw. Technol.*, vol. LT-5, no. 5, pp. 660–667, May 1987.

Nima Zareian was born in Tehran, Iran, in April 1983. He received the B.S. degree in electrical engineering from Isfahan University of Technology, Isfahan, Iran, in 2005. He is currently working toward the M.S. degree in electrical engineering at Sharif University of Technology, Tehran, Iran.

His current research interests include photonics and periodic structures.

Peyman Sarrafi was born in Tehran, Iran, in September 1983. He received the B.S. degree in electrical engineering from Shahid Beheshti University, Tehran, Iran, in 2005. He is currently working towards the M.S. degree in electrical engineering at Sharif University of Technology, Tehran, Iran.

His current research interests include photonics and bandgap materials.

Khashayar Mehrany was born in Tehran, Iran, on September 16, 1977. He received the B.Sc., M.Sc., and Ph.D. (*magna cum laude*) degrees from Sharif University of Technology, Tehran, Iran, in 1999, 2001, and 2005, respectively, all in electrical engineering.

Since then, he has been an Assistant Professor with the Department of Electrical Engineering, Sharif University of Technology. His research interests include photonics, semiconductor physics, nanoelectronics, and numerical treatment of electromagnetic problems. He is author and coauthor of more than 45 scientific articles in international journals and conferences.

Bizhan Rashidian received the B.Sc. and M.Sc. (highest hons) degrees from Tehran University, Tehran, Iran, and the Ph.D. degree from the Georgia Institute of Technology, Atlanta, in 1987, 1989, and 1993, respectively, all in electrical engineering.

Since 1994, he has been with the Department of Electrical Engineering at Sharif University of Technology, where he is now a Professor and the Founding Director of the Microtechnology and Photonics Laboratories. His active research areas include optics, micromachining, microelectronics, and ultrasonics.